SYSTEMATIC AEROSOL CHARACTERIZATION BY COMBINING UV AEROSOL INDICES WITH TRACE GAS CONCENTRATIONS

M. J. M. Penning de Vries[1], S. Beirle[1], C. Hörmann[1], J. W. Kaiser[1,2], L. G. Tilstra[3], O. N. E. Tuinder[3], P. Stammes[3], and T. Wagner[1]

[1] Max Planck Institute for Chemistry, Mainz, Germany
[2] European Centre for Medium-range Weather Forecast (ECMWF), Reading, UK
[3] Royal Netherlands Meteorological Institute (KNMI), De Bilt, Netherlands
Contact: marloes.penningdevries@mpic.de

Abstract

Knowledge of aerosol type or source is of importance for the calculation of aerosol radiative effects, for the development and monitoring of mitigation strategies, and for the construction of climatologies of aerosol optical properties (needed for, e.g., aerosol retrieval). Our Global Aerosol Classification Algorithm, GACA, examines aerosol properties (MODIS Aerosol Optical Thickness (AOT) and extinction Ångström exponent, GOME-2 UV Aerosol Indices) and trace gas column densities (NO_2, HCHO, SO_2 from GOME-2, and CO from MOPITT) measured from space in order to classify different aerosol types and dominating source types.
Using GACA, global maps of dominant aerosol type and main source type were constructed for each season. The seasonal cycles of both aerosol type and source were also studied in more detail for several 5° x 5° regions. The agreement with aerosol types from ECMWF's MACC model is generally good for urban/industrial (SO_4) aerosols and biomass burning smoke, but the variability (yearly and/or seasonal) is often not well captured by MACC. The amount of mineral dust outside of the dust belt appears to be overestimated, and the abundance of secondary organic aerosols is severely underestimated in comparison with GACA.
The presented study is of exploratory nature, but we show that our method is well suited to evaluate climate models by comparing measured and modeled aerosol type and source instead of focusing on a single parameter, e.g. AOT.

INTRODUCTION

The uncertainties in global distribution of aerosol loading have become progressively smaller during the past decade owing to dedicated satellite-borne aerosol instruments like MODIS and MISR. However, for many applications the aerosol amount tells only half of the story: to determine aerosol radiative effects, to study the interaction between different aerosols and clouds, but also for the development of mitigation strategies it is crucial to additionally know the aerosol type or source (e.g., Stocker et al., 2013). For remote sensing retrievals themselves, aerosol optical properties or some constraints on particle type are also needed in the inversion process.
In a recent publication, Veefkind and co-workers showed that the presence of significant correlation of AOT with trace gas concentrations, notably NO_2 and HCHO, is an indication of the main source of aerosols (Veefkind et al., 2011). In the present exploratory study, we take these findings a step further and integrate them into an algorithm to determine the main aerosol type and its source on a global scale. Our Global Aerosol Characterization Algorithm, GACA, combines the extinction Ångström exponent (EAE) from MODIS and GOME-2 UV Aerosol Index (UVAI) to determine an aerosol type based on its size and absorption. In a second step, means of trace gas vertical column density (VCDs of NO_2, HCHO, SO_2, and CO), fire counts and their respective correlations with AOT are computed for grid boxes of 2° x 2° resolution. The most likely aerosol source is subsequently selected based on a series of threshold tests.
GACA results are compared to aerosol composition from ECMWF's MACC-II (Monitoring Atmospheric Composition and Climate – Interim Implementation) model on a global and regional scale.

In this paper we present global maps of aerosol type and main source, as well as the regional seasonal cycles of aerosol type and source in four regions. Despite the exploratory nature of this study, we find good agreement between results from GACA and MACC. Several important discrepancies between the data sets are discussed.

DATA SETS

Several data sets, each spanning four years (2007-2010) from three different instruments were used in this study. The data sets are summarized below; for further information we refer the reader to the cited literature or the websites mentioned in the acknowledgements.
Monthly mean values of AOT from MODIS-AQUA collection 5.1 (Remer et al., 2005; Levy et al., 2007) at 1°x 1° resolution were obtained from LAADS web. For bright surfaces (mainly deserts), the Deep Blue product (Hsu et al., 2004) was used. MODIS AOT is given at 550 nm; monthly mean EAE was calculated from mean AOT at 470 nm and 660 nm. EAE was favored over fine-mode fraction (FMF) as a measure of aerosol size because FMF is not determined by the Deep Blue algorithm.
UVAI is a qualitative indicator of aerosols. It consists of the Absorbing Aerosol Index (AAI), which is a measure of aerosols that absorb UV radiation (e.g., Torres et al., 1998; de Graaf et al., 2005), and of the SCattering Index (SCI), which can be used for the detection of non-absorbing aerosols (Penning de Vries et al., 2009). The UVAI are a complex function of AOT, aerosol absorption, and layer altitude, and using them in a quantitative sense is not straightforward; however, in combination with information on aerosol abundance (i.e., AOT), UVAI give useful information on aerosol absorption. Here, the operational AAI from TEMIS was used. Because both AAI and SCI are used in GACA, the term UVAI will be used throughout this document.
Daily Vertical Column Densities (VCDs) of GOME-2 tropospheric NO_2 (Boersma et al., 2004) and HCHO (De Smedt et al., 2012) were obtained from TEMIS; VCDs of SO_2 were determined from GOME-2 data using the algorithm developed at our institute, described in (Hörmann et al., 2013). The trace gas data were gridded to 1°x 1° and averaged for each month from 2007-2010. After cloud filtering (effective cloud fraction below 0.2), the data were gridded on a 1°x 1° resolution and averaged over one month.
Version-5 MOPITT CO total vertical column density data from the combined near- and thermal infrared (NIR-TIR) algorithm (Deeter et al., 2003) were obtained from NASA. The CO difference (value minus background, denoted as ΔCO) is used instead of the absolute value obtained by subtracting a background column equal to the median of the data within each 5° latitude band. This procedure is needed due to the long life time of CO and allows the use of a single CO threshold value throughout the year and for the whole globe.
Gridded monthly total fire counts were obtained from MODIS-AQUA (Giglio et al., 2003).
MACC-II reanalysis data, comprising monthly mean AOT of five aerosol components (black carbon, desert dust, organic matter, sulfate, and sea salt) were obtained from ECMWF at 1°x 1° resolution. Aerosol abundance is estimated by MACC-II by combining information from models and MODIS observations of AOT (Benedetti et al., 2009; Inness et al., 2013).

GLOBAL AEROSOL CHARACTERIZATION ALGORITHM

Data selection

The first step in GACA is the selection of data for each grid box. Assuming the resolution of the final product is to be 2°x 2°, and the input monthly mean maps (of AOT, UVAI, EAE, fire counts and trace gas column densities) have a resolution of 1°x 1°, each grid box on the globe contains 4 data points per month. To improve statistics and stability of the algorithm, the data are grouped by season (12 data points) and four years of data are used (48 data points). Grid boxes in which the monthly mean AOT never exceeds 0.05 are removed, as it is assumed that they cannot be reliably classified. The data set is subsequently screened for missing values and outliers; the latter because the intention is to build a climatology, which should not be influenced by exceptional events.

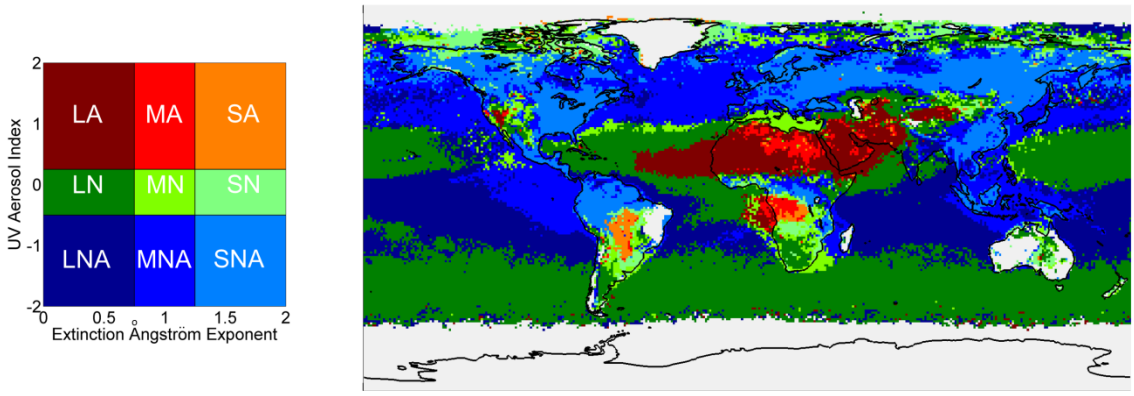

Figure 1: **Separation into aerosol types based on absorption (UVAI) and size (EAE). Left - Aerosol types: LA, large absorbing; MA, medium-size absorbing; SA, small absorbing; LN, large neutral; MN, medium-size neutral; SN, small neutral; LNA, large non-absorbing; MNA, medium-size non-absorbing; SNA, small non-absorbing.**
Right - Global aerosol type distribution according to GACA for June-August 2007-2010 at 2° x 2° resolution. Aerosol types are color-coded according to size (larger sizes have darker hues) and absorption (non-absorbing in blue, neutral in green, absorbing in red), as in the scheme at left.

GACA-type

Each point of the filtered data set is assigned one of nine aerosol types based on its UVAI and EAE values. In this study, aerosol types are defined by their size - small (S), medium (M), and large (L) - and the amount of aerosol absorption - non-absorbing (NA), neutral (N), or absorbing (A) - as shown in the left panel of Fig.1. For each grid box, the fraction of points belonging to each aerosol type is computed and the most frequently observed type, weighted by AOT, is assumed to be the dominant type.

GACA-source

The source is deduced from the aerosol type, from the mean values of trace gas column densities and fire counts, and from the correlation coefficient between AOT and trace gas abundances (or UVAI). This is done once for all data within a 2° x 2° grid box, and once again for each aerosol type (e.g. MA or SMA) that occurs in the grid box separately. For the calculation of the means and correlation coefficients, all valid data points within a grid box are included with a minimum of 5 points. The tests performed by GACA-source are based on thresholds of which the values were chosen empirically and are given in Table 1.

Table 1: **Ranges and thresholds used in GACA.**

Variable	Nominal range	Thresholds	GACA step
AOT	0 - 3	0.05 , 0.15	Filtering, Source
EAE	0 - 2	0.75 and 1.25	Aerosol type
UVAI	-2.5 - 2.5	-0.5 and 0.25	Aerosol type
Fire counts	0 - 500	50	Source
NO_2 VCD	$0 – 10x10^{15}$	$1x10^{15}$	Source
HCHO VCD	$0 – 25x10^{15}$	$5x10^{15}$	Source
SO_2 VCD	$0 – 20x10^{15}$	$2x10^{15}$	Source
ΔCO VCD	$0 – 4x10^{17}$	$3x10^{17}$	Source
HCHO:NO_2 ratio	0 – 100	4	Source
Correlation coefficient, R^2	0 - 1	0.25	Source

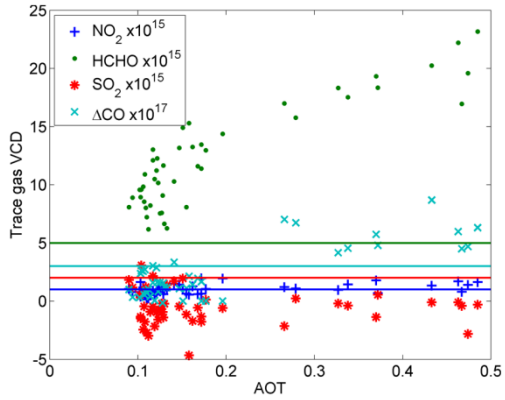

Figure 2: **Relationship between AOT and trace gas VCDs for a 2°x 2° region in South America (around 5°S, 61°W) for July-August 2007-2010. Symbols depict monthly means of NO_2 (blue +), HCHO (green dots), SO_2 (red *) and ΔCO (light blue x) together with their respective thresholds (colored horizontal lines).**

Figure 2 illustrates the GACA-source procedure for a 2° x 2° region in South America (5°S / 61° W) during the biomass burning season (June-August, 2007-2010). The trace gas columns are shown together with their respective thresholds, so that if the values fall below the corresponding threshold line the trace gas is assumed not to be associated with the local aerosols. For the selected grid box, mean NO_2, HCHO, and ΔCO are enhanced and their correlation with AOT is good enough (R^2>0.25). The level of SO_2 is close to or even below the detection limit, leading to scatter of SO_2 data and negative values. The aerosol source is assigned according to the criteria and in the sequence given in Table 2; once for each subset of data belonging to a certain aerosol type, and once for all data within the grid box. For the data shown in Fig. 2, biomass burning (BB) is determined to be the main source: the AOT-weighted dominating aerosol type is SNA, but the absorbing aerosol criterion is met (good correlation between AOT and UVAI) and the combination with high mean ΔCO leads to the assignment of BB.

Table 2: **Criteria for the assignment of aerosol source. The letters in brackets indicate either mean values (m), the correlation coefficient (c), or both (mc). Note that the assignment sequence is from top to bottom.**

Source	Short	Types	Over threshold	Below threshold	Other criteria
Biomass burning	BB	All	CO(mc) and/or HCHO(mc) and/or fire(m)		SA type always, absorbing aerosol criterion*
Mineral dust	DD	MA, LA		CO(c) and NO_2(m) and HCHO(m) and SO_2(m)	LA type always
Secondary biogenic	BIO	SNA	HCHO(m) and HCHO:NO_2		
Secondary urban	URB	All but SA, MA, LA	NO_2(m)	HCHO:NO_2	
Aged	AGED	All but SA, MA, LA	CO(m)	NO_2(m)	
Volcanic sulfate	VOG	All but SA, MA, LA	SO_2(mc)	NO_2(m) and CO(m)	
Sea salt	SS	MNA, MN, LNA ,LN		All trace gas means	AOT<0.15
Undefined mixture	MIX	All but SA, LA			Unassigned boxes with AOT>0.05
Not analyzed	na				Boxes with AOT<0.05 or gaps

***Absorbing aerosol criterion: high mean UVAI and/or good, positive correlation between AOT and UVAI.**

RESULTS

Aerosol type

We applied GACA-type to the data set for the four seasons of 2007-2010 to study aerosol properties globally; the resulting map of dominating aerosol type in summer on a 1° x 1° resolution is shown in

the right panel of Figure 1. The dust belt (at around 10°N-40°N) is dominated by large particles (dark hues) with strong to moderate absorption (red and green tones). Smoke plumes from central Africa consist mostly of small to medium-size absorbing particles (orange and red), although there appears to be a significant contribution from large absorbing (LA) particles. Close inspection reveals a discrepancy between EAE and FMF, both measured by MODIS, in this region: EAE <0.75, pointing to the presence of coarse particles, but FMF >>0.5, indicating a high fraction of small particles. It is unclear at the moment what causes this discrepancy; we speculate that the presence of the persistent stratocumulus deck under the aerosol layer has an influence.
North America, Europe and large parts of Asia are dominated by small, non-absorbing aerosols (light blue). Over ocean, particularly in the southern oceans, large particles (dark blue and green) dominate. Light gray areas denote regions where no AOT data were available (e.g. due to cloud cover) or where monthly mean AOT did not exceed 0.05 within the studied period. The biomass burning season in South America, which starts in July-August and peaks in September-October, has a very different signature than that in Central/South Africa: the particles are smaller and appear less absorbing. This is probably a consequence of the difference in fuel type, but is also caused by the larger cloud cover in South America, which leads to lower UVAI values and to more data gaps in the trace gas products.

Aerosol source

The results from a run of GACA-source with data from June-August 2007-2010 are shown in the form of a global map of 2° x 2° resolution in the left panel of Fig. 3. Most of the continental northern hemispheric aerosols are of urban/industrial origin (URB, dark blue), except in the South-Arabian peninsula and Northwestern China, where mineral dust (DD, red) predominates. Absorbing particles emitted by biomass burning (BB, brown) can be found in Central-South Africa and South America. Aside from producing BB emissions, Southern Africa and the forested part of South America are a large source of secondary biogenic particles (BIO, dark green). Aged aerosols (AGED, blue-gray) can be seen in the outflow from Northeast Asia (China) and in the air masses transported from equatorial Africa over the Atlantic. Most aerosols over oceans are classified as sea salt (SS, light blue), although some mixtures of unknown composition (MIX, gray) are found in the Asian outflow over the Pacific and the African outflow over the Atlantic. A conspicuous VOG plume is seen emerging from Hawaii and is mainly due to prodigious degassing in March-October 2008 by the Kilauea volcano (19.4°N/155.3°W) (e.g., Beirle et al., 2014).

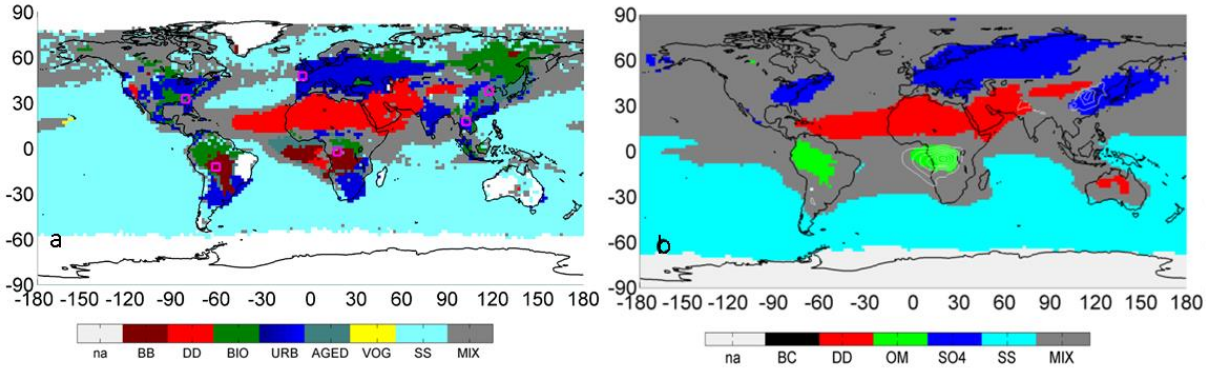

Figure 3: **Global main aerosol source type distribution according to GACA (a) and MACC (b). Data are from June-August 2007-2010. Aerosol source type abbreviations are given in Table 2 for GACA; Aerosol types for MACC are: black carbon (BC), mineral dust (DD), organic matter (OM), sulfate (SO4), sea salt (SS), and mixture (MIX). Light gray areas (na) are not analyzed due to lack of data or too small mean AOT. As BC does not dominate anywhere, contours show mean BC amount (AOT 0.01-0.1) to indicate regions affected by smoke; see text for details.**

Comparison with MACC

Main aerosol types were obtained from MACC model data for all seasons of 2007-2010 on a 2° x 2° resolution to improve the comparison with the GACA-source results. The dominating aerosol component for summer (June-August) is shown in the right panel of Fig. 3. AOT due to BC are additionally shown in contours (AOT=0.01-0.1) to indicate the regions affected by biomass burning, as BC constitutes only a small fraction of aerosol emissions by fires. The aerosol type is set to MIX when none of the aerosol components contributes more than 50% of AOT. It must be noted that MACC data are inherently different from GACA data in that each data point contains contributions of each aerosol

component (BC, OM, DD, SO4, SS); for aerosol characterization by GACA, only one aerosol type and source can be determined per data point at most. Nevertheless, at a first glance, the agreement between GACA-source and MACC is quite good: the general patterns of DD and SO4 (or URB) agree well. The location and extent of biomass burning regions also agree well, although MACC does not show BC in South America in summer, where GACA sees a lot of BB. The main sources of BIO (or OM) agree in GACA and MACC, but the source in Southeast USA is missed by MACC. The differences between MACC and GACA will be discussed in more detail in the following section, where regional seasonal cycles are investigated.

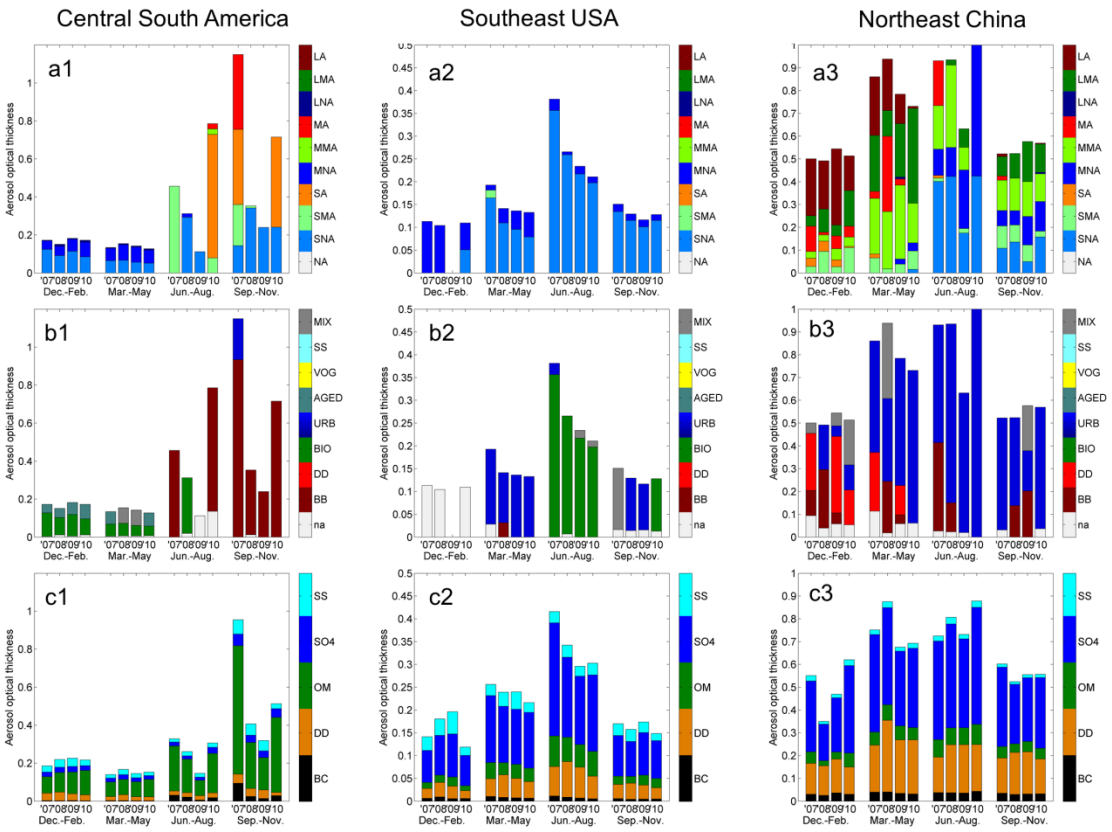

Figure 4: **Seasonal cycles of global aerosol and type and source according to GACA and MACC for 5° x 5° regions in central South America (CSA, 12.5°S/62.5°W),Southeastern USA (SEU, 32.5°N/82.5°W), and Northeastern China (NEC, 32.5°N/117.5°E). Data are grouped into four seasons and separated by year. Panels a1-3: mean AOT contribution of each aerosol type; b1-3: mean AOT contribution of aerosol source (determined from each aerosol type); c1-3: mean AOT contribution of aerosol type from MACC. Aerosol type abbreviations are given in Fig. 1, source types in Table 2, and MACC aerosol types in Fig. 3.**

Regional seasonal cycles

Three 5° x 5° regions were selected for the study of the seasonal cycle: Central South America (CSA), Southeastern USA (SEU), and Northeastern China (NEC); the regions are shown as pink boxes in the left panel of Fig. 3. For each season and each year (2007-2010), the frequency of occurrence of aerosol types is shown in panels a1-3 of Fig.4. Panels b1-3 show the AOT contribution of each GACA source type, determined from each aerosol type separately, is presented. Finally, panels c1-3 display MACC aerosol types.

The first region, CSA (first column of Fig. 4), is characterized by seasonal biomass burning. The fire season starts in late summer; the highest number of fire counts is usually found in fall (September-November). The high year-to-year variability of biomass burning is clearly reflected in all three panels. Both GACA and MACC ascribe the larger part of AOT in winter and spring to organic aerosols (BIO and OM in GACA and MACC, respectively). Although the DD contribution in MACC appears to be somewhat high (no DD is detected by GACA), the agreement between GACA and MACC is good for this example.

The region SEU is affected most by non-absorbing aerosols (second column of Fig. 4). Throughout most of the year, aerosols over Southeastern USA are of urban/industrial origin (URB and SO4 for GACA and MACC, respectively). GACA attributes nearly all AOT to BIO in summer, in agreement with previous studies that found secondary organic aerosols to be the dominating source in this region (e.g., Goldstein et al., 2009). MACC, on the other hand, does not include secondary organic aerosols and thus only shows a slight increase in OM relative to the other seasons. The contribution of dust to the aerosol mixture appears to be too big in comparison to GACA results.
The third column shows the seasonal cycle of Northeastern China. The mean AOT in this region is greater than 0.5 throughout the year for each year from 2007-2010. Most of the AOT can be attributed to aerosols of anthropogenic origin (URB and SO4), but a large fraction is caused by mineral dust (DD) transported from deserts in Mongolia, northern China, and Kazakhstan, especially in winter and spring. In view of their sizes (medium to large), at least some of the aerosols characterized as BB by GACA are probably polluted dust or dust in the presence of pollution (i.e. NO_2, HCHO, SO_2 and CO). Even so, the variability of the seasonal cycle of DD appears to be underestimated by MACC. The amount of BC modeled by MACC is as high as for central South America in the biomass burning season (except in the fall of 2007, see panel c1), which explains the high levels of aerosol absorption found by GACA for Northeastern China.

CONCLUSIONS

Aerosols and trace gases are often co-located, or even correlated, because they are (1) emitted by the same sources, e.g. in the case of biomass burning smoke; (2) formed from the same precursor, e.g. secondary organic aerosols; or (3) formed from those trace gases in the atmosphere, e.g. sulfate aerosols. We present a first attempt at exploiting this fact for the characterization of aerosol type - and, hence, aerosol properties - from satellite observations. In this paper, we introduce a strategy for the systematic characterization of aerosols using the combination of AOT and EAE from MODIS with UVAI and trace gas columns (NO_2, HCHO, and SO_2) from GOME-2, CO columns from MOPITT, and MODIS fire counts.
The obtained global yearly and seasonal maps are in good agreement with MACC model data, although systematic differences were also found: more desert dust and less secondary organic aerosols are found by MACC than by GACA. This demonstrates the potential of our method - combining aerosol and trace gas data - to evaluate and investigate aerosol treatment (parameterization, sources, transport, aging and removal processes) in climate models.
We find that a rather simple algorithm suffices for very plausible results that are quite robust with respect to aerosol and trace gas data sets and choice of cloud fraction thresholds. We emphasize, however, that the presented study is exploratory in nature and that there is much room for improvement of the algorithm.
With the upcoming new generation of space-based DOAS instruments with high spatial resolution, in particular TROPOMI (on the polar-orbiting Sentinel 5p platform) and the geo-stationary Sentinel 4, more (cloud-free) data will be available for studies as presented here. With such instruments, global aerosol type maps with even higher spatial and temporal resolution become feasible. This is of interest to modelers, who can use the information to verify emissions and aerosol processes, and for scientists working to update aerosol climatologies used in the retrieval of AOT (e.g., MODIS) or trace gas VCDs.

ACKNOWLEDGEMENTS

We thank K. Mies for help with the MPIC SO2 retrieval. The O3M SAF is acknowledged for funding visiting scientist project O3-VS10-01 (M. P.d.V.) and for GOME-2 AAI; ESA and EUMETSAT for GOME-2 Level-1 data; NASA for MODIS AOT (http://ladsweb.nascom.nasa.gov/index.html), fire counts (https://earthdata.nasa.gov/data/near-real-time-data/about-lance/data-centers/modaps) and MOPITT CO (https://subset.larc.nasa.gov/mopitt/) data; ECMWF for MACC reanalysis data (http://apps.ecmwf.int/datasets/data/macc_reanalysis/). J. W. Kaiser was supported by the FP7 EU project MACC-II (grant agreement no. 283576). We acknowledge the free use of GOME-2 tropospheric NO2 and HCHO column data and AAI from www.temis.nl .

REFERENCES

Beirle, S., Hörmann, C., Penning de Vries, M., Dörner, S., Kern, C. and Wagner, T.: Estimating the volcanic emission rate and atmospheric lifetime of SO2 from space: a case study for Kīlauea volcano, Hawai`i, Atmos. Chem. Phys., 14(16), 8309–8322, doi:10.5194/acp-14-8309-2014, 2014.

Benedetti, A., Morcrette, J.-J., Boucher, O., Dethof, A., Engelen, R. J., Fisher, M., Flentje, H., Huneeus, N., Jones, L., Kaiser, J. W., Kinne, S., Mangold, A., Razinger, M., Simmons, A. J. and Suttie, M.: Aerosol analysis and forecast in the European Centre for Medium-Range Weather Forecasts Integrated Forecast System: 2. Data assimilation, J. Geophys. Res., 114(D13), D13205, doi:10.1029/2008JD011115, 2009.

Boersma, K. F., Eskes, H. J. and Brinksma, E. J.: Error analysis for tropospheric NO2 retrieval from space, J. Geophys. Res., 109(D4), D04311, doi:10.1029/2003JD003962, 2004.

Deeter, M. N., Emmons, L. K., Francis, G. L., Edwards, D. P., Gille, J. C., Warner, J. X., Khattatov, B., Ziskin, D., Lamarque, J.-F., Ho, S.-P., Yudin, V., Attié, J.-L., Packman, D., Chen, J., Mao, D. and Drummond, J. R.: Operational carbon monoxide retrieval algorithm and selected results for the MOPITT instrument, J. Geophys. Res., 108(D14), 4399, doi:10.1029/2002JD003186, 2003.

De Smedt, I., Van Roozendael, M., Stavrakou, T., Müller, J.-F., Lerot, C., Theys, N., Valks, P., Hao, N. and van der A, R.: Improved retrieval of global tropospheric formaldehyde columns from GOME-2/MetOp-A addressing noise reduction and instrumental degradation issues, Atmos. Meas. Tech., 5(11), 2933–2949, doi:10.5194/amt-5-2933-2012, 2012.

Giglio, L., Descloitres, J., Justice, C. O. and Kaufman, Y. J.: An Enhanced Contextual Fire Detection Algorithm for MODIS, Remote Sensing of Environment, 87(2–3), 273–282, doi:10.1016/S0034-4257(03)00184-6, 2003.

Goldstein, A. H., Koven, C. D., Heald, C. L., and Fung, I. Y.: Biogenic carbon and anthropogenic pollutants combine to form acooling haze over the southeastern United States, PNAS, 106,8835–8840, doi:10.1073/pnas.0904128106, 2009.

de Graaf, M., Stammes, P., Torres, O., and Koelemeijer, R.B.A.: Absorbing Aerosol Index - Sensitivity analysis, application to GOME and comparison with TOMS, J. Geophys. Res., 110, D01202, doi:10.1029/2004JD005178, 2005.

Hörmann, C., Sihler, H., Bobrowski, N., Beirle, S., Penning de Vries, M., Platt, U., and Wagner, T.: Systematic investigation of bromine monoxide in volcanic plumes from space by using the GOME-2 instrument, Atmos. Chem. Phys., 13, 4749-4781, doi:10.5194/acp-13-4749-2013, 2013.

Inness, A., Baier, F., Benedetti, A., Bouarar, I., Chabrillat, S., Clark, H., Clerbaux, C., Coheur, P., Engelen, R. J., Errera, Q., Flemming, J., George, M., Granier, C., Hadji-Lazaro, J., Huijnen, V., Hurtmans, D., Jones, L., Kaiser, J. W., Kapsomenakis, J., Lefever, K., Leitão, J., Razinger, M., Richter, A., Schultz, M. G., Simmons, A. J., Suttie, M., Stein, O., Thépaut, J.-N., Thouret, V., Vrekoussis, M., Zerefos, C. and the MACC team: The MACC reanalysis: an 8 yr data set of atmospheric composition, Atmos. Chem. Phys., 13(8), 4073–4109, doi:10.5194/acp-13-4073-2013, 2013.

Hsu, N. 495 C., Tsay, S.-C., King,M. D. and Herman, J. R.: Aerosol properties over bright-reflecting source regions, IEEE Trans. Geosci. Rem. Sens., 42(3), 557–569, doi:10.1109/TGRS.2004.824067,2004.

Levy, R. C., Remer, L. A., Mattoo, S., Vermote, E. F. and Kaufman, Y. J.: Second-generation operational algorithm: Retrieval of aerosol properties over land from inversion of Moderate Resolution Imaging Spectroradiometer spectral reflectance, J. Geophys. Res., 112(D13), D13211, doi:10.1029/2006JD007811, 2007.

Penning de Vries, M.J.M., Beirle, S., and Wagner, T.: UV Aerosol Indices from SCIAMACHY: introducing the SCattering Index (SCI), Atmos. Chem. Phys., 9, 9555-9567, doi:10.5194/acp-9-9555-2009, 2009.

Remer, L. A., Kaufman, Y. J., Tanre, 535 D., Mattoo, S., Chu, D. A., Martins, J. V., Li, R.-R., Ichoku, C., Levy, R. C., Kleidman, R. G., Eck, T. F., Vermote, E. and Holben, B. N.: The MODIS Aerosol Algorithm, Products, and Validation, J. Atmos. Sci., 62(4), 947–973, doi:10.1175/JAS3385.1, 2005.

Stocker, T.F., et al.: Technical Summary in Climate Change 2013: The Physical Science Basis. Contribution of Working Group I to the Fifth Assessment Report of the Intergovernmental Panel on Climate Change [Stocker, T.F., Qin, D., Plattner, G.-K., Tignor, M., Allen, S.K., Boschung, J., Nauels, A., Xia, Y., Bex, V., and Midgley, P.M. (eds)]. Cambridge University Press, Cambridge, UK, and New York, USA, 2013.

Torres, O., Bhartia, P.K., Herman, J.R., Ahmad, Z., and Gleason, J.: Derivation of aerosol properties from satellite measurements of backscattered ultraviolet radiation: Theoretical basis, J. Geophys. Res., 103(D14), 17099-17110, 1998.

Veefkind, J. P., Boersma, K. F., Wang, J., Kurosu, T. P., Krotkov, N., Chance, K. and Levelt, P. F.: Global satellite analysis of the relation between aerosols and short-lived trace gases, Atmos. Chem. Phys., 11(3), 1255–1267, doi:10.5194/acp-11-1255-2011, 2011.